

TRANSACTIONS OF
K.C. WONG EDUCATION FOUNDATION
SUPPORTED LECTURES

王宽诚教育基金会

学术讲座汇编

主 编 钱伟长

· 29 ·

2008

上海大学出版社

王宽诚教育基金会

学术讲座汇编

(第 29 集)

主编 钱伟长

上海大学出版社

图书在版编目(CIP)数据

王宽诚教育基金会学术讲座汇编. 第29集/钱伟长主编.
—上海: 上海大学出版社, 2008. 12
ISBN 978-7-81118-355-9

I. 王… II. 钱… III. ① 社会科学—文集 ② 自然科学—文集 IV. Z427

中国版本图书馆 CIP 数据核字(2008)第 169872 号

王宽诚教育基金会

学术讲座汇编(第29集)

钱伟长 主编

上海大学出版社出版发行

(上海市上大路99号 邮政编码200444)

(<http://www.shangdapress.com> 发行热线 66135110)

出版人: 姚铁军

*

南京展望文化发展有限公司排版

上海第二教育学院印刷厂印刷

开本 787×1092 1/16 彩插1 印张 13.5 字数 320 千字

2008年12月第1版 2008年12月第1次印刷

印数: 1~850册

ISBN 978-7-81118-355-9/Z·017

王宽诚教育基金会简介

王宽诚先生(1907—1986)为香港著名爱国人士,热心祖国教育事业,生前为故乡宁波的教育事业做出积极贡献。1985年独立捐巨资创建王宽诚教育基金会,其宗旨在于为国家培养高级技术人才,为祖国四个现代化效力。

王宽诚先生在世时聘请海内外著名学者担任基金会考选委员会和学务委员会委员,共商大计,确定采用“送出去”和“请进来”的方针,为国家培养各科专门人才,提高内地和港澳高等院校的教学水平,资助学术界人士互访以促进中外文化交流。在此方针指导下,1985、1986两年,基金会在国家教委支持下,选派学生85名前往英、美、加拿大、德国、瑞士和澳大利亚各国攻读博士学位,并计划资助内地学者赴港澳讲学,资助港澳学者到内地讲学,资助美国学者来国内讲学。正当基金会事业初具规模、蓬勃发展之时,王宽诚先生一病不起,于1986年年底逝世。这是基金会的重大损失,共事同仁,无不深切怀念,不胜惋惜。

1987年起,王宽诚教育基金会继承王宽诚先生为国家培养高级技术人才的遗愿,继续对中国内地、台湾及港澳学者出国攻读博士学位、博士后研究及学术交流提供资助。委请国家教育部、中国科学院和上海大学校长钱伟长教授等逐年安排资助学术交流的项目。相继与(英国)皇家学会、法国科研中心、德国学术交流中心、法国高等科学研究院等著名欧洲学术机构合作,设立“王宽诚(英国)皇家学会奖学金”、“王宽诚法国科研中心奖学金”、“王宽诚德国学术交流中心奖学金”、“王宽诚法国高等科学研究院奖学金”,资助具有副教授或同等职称以上的中国内地学者前往英国、法国、德国等地的高等学府及科研机构进行为期2至12个月之博士后研究。

王宽诚教育基金会过去和现在的工作态度一贯以王宽诚先生倡导的“公正”二字为守则,谅今后基金会亦将秉此行事,奉行不辍,借此王宽诚教育基金会《学术讲座汇编》出版之际,特简明介绍如上。王宽诚教育基金会日常工作繁忙,基金会各位董事均不辞劳累,做出积极贡献。

钱 伟 长

二〇〇八年十二月

前 言

王宽诚教育基金会是由已故全国政协常委、香港著名工商企业家王宽诚先生(1907—1986)出于爱国热忱,出资一亿美元于1985年在香港注册登记创立的。

1987年,基金会开设“学术讲座”项目,此项目由当时的全国政协委员、历任第六、七、八、九届全国政协副主席、著名科学家、中国科学院院士、上海大学校长、王宽诚教育基金会贷款留学生考选委员会主任委员兼学务委员会主任委员钱伟长教授主持。由钱伟长教授亲自起草设立“学术讲座”的规定,资助内地学者前往香港、澳门讲学,资助美国学者来中国讲学,资助港澳学者前来内地讲学,用以促进中外学术交流,提高内地及港澳高等院校的教学质量。

本汇编收集的文章,均系各地学者在“学术讲座”活动中的讲稿,文章内容有科学技术,有历史文化,有经济专论,有文学,有宗教和中国古籍研究等。本汇编涉及的学术领域颇为广泛,而每篇文章都有一定的深度和广度,分期分册以《王宽诚教育基金会学术讲座汇编》的名义出版,并无偿分送国内外部分高等院校、科研机构 and 图书馆,以广流传。

王宽诚教育基金会除资助“学术讲座”学者进行学术交流之外,在钱伟长教授主持的项目下,还资助由国内有关高等院校推荐的学者前往欧、美、亚、澳等参加国际学术会议,出访的学者均向所出席的会议提交论文,这些论文亦颇有水平,本汇编亦将其收入,以供参考。

王宽诚教育基金会学务委员会

凡 例

（一）编排次序

本书所收集的王宽诚教育基金会学术讲座的讲稿及由王宽诚教育基金会资助学者赴欧、美、亚、澳等参加国际学术会议的论文均按照文稿日期先后或文稿内容编排刊列,不分类别。

（二）分期分册出版并作简明介绍

因文稿较多,为求便于携带,有利阅读与检索,故分期分册出版,每册约 150 页至 200 页不等。为便于读者查考,每篇学术讲座的讲稿均注明作者姓名、学位、职务、讲学日期、地点、访问院校名称。内地及港、澳学者到欧、美、澳及亚洲的国家和地区参加国际学术会议的论文均注明学者姓名、参加会议的名称、时间、地点和推荐的单位。上述两类文章均注明由王宽诚教育基金会资助字样。

（三）文字种类

本书为学术性文章汇编,均以学术讲座学者之讲稿原稿或参加国际学术会议者向会议提交的论文原稿文字为准,原讲稿或论文是中文的,即以中文刊出,原讲稿或论文是外文的,仍以外文刊出。

目 录 CONTENTS

Analysis on Interface Failure Mechanism of Reinforced Concrete Continuous Beam
Strengthened by FRP YUAN Hong LIN Zi-feng (1)

Design of Single-phase Shunt Active Power Filter Based on ANN
..... DAI Wen-jin HUANG Tai-yang (13)

The Influence of Culture on Enterprise Portal Design in a Global Environment
..... FENG Xiu-zhen, EHRENHARD Michel L, HICKS Jeff N, HOU Yi-bin (22)

Study on Multi-Production Process Based on Recoveries of SO₂ and CO₂ from Flue
Gas ZHU Jia-hua, LIU Zhuo-qu, XIA Su-lan (31)

Effects of High Magnetic Fields on Solidification in Mn-89.7% Sb Alloy
..... WANG Qiang, LIU Tie, GAO Ao, WANG Chun-jiang,
WEI Ning, HE Ji-cheng (39)

Sintering and Optimizing Design of the Microstructure of Sol-Gel Derived BaTiO₃
Ceramics by Artificial Neural Networks FAN Hui-qing, LIU Lai-jun (46)

Investigation on the Definition and Digital Algorithm of Instantaneous Dielectric Loss
Factor LI Qing-min, ZHANG Li (58)

Repair and Strengthening of Two-way Curved Arch Bridge
..... PING Shang-guan, ZHUO Wei-dong (70)

《元典章》整理的回顾与展望 张 帆 (77)

数字地形分析及其地理学应用..... 周启鸣 (82)

Remote Sensing Change Detection Zhou Qi-ming (104)

市场转型,教育扩张与教育机会的公平性研究..... 吴晓刚 (127)

市场转型与社会分层:研究展望 吴晓刚 (140)

比较社会分层与流动研究的新进展 吴晓刚 (149)

How to Write a xxx Research Paper? 吴晓刚 (160)

Nano Calcium Phosphate Particles in Biomineralization TANG Rui-kang (170)

Interaction of overlay Networks: Properties and Control LUI John C S (183)

编后记..... (201)

Analysis on Interface Failure Mechanism of Reinforced Concrete Continuous Beam Strengthened by FRP

YUAN Hong * LIN Zi-feng

(Department of Mechanics and Civil Engineering, Jinan University,
Guangzhou 510062, P. R. China)

Abstract: Fiber reinforced polymer (FRP) composites are increasingly being used for the repair and strengthening of deteriorated concrete structural components through adhesive bonding of prefabricated strips/plates and the wet lay-up of fabric. Interfacial bond failure modes have attracted the attention of the researchers because of the importance. The objective of the present study is to analyse the interface failure mechanism of reinforced concrete continuous beam strengthened by FRP. An analytical solution has been firstly presented to predict the entire debonding process of the model. The realistic bi-linear bond-slip interfacial law was adopted to study this problem. The crack propagation process of the loaded model was divided into four stages (elastic, elastic-softening, elastic-softening-debonded and softening-debonded stage). Among them, elastic-softening-debonded stage has four sub-stages. The equations are solved by adding suitable stress and displacement boundary conditions. Finally, critical value of bond length is determined to make the failure mechanism in the paper be effect by solving the simultaneously linear algebraic equations. The interaction of upper and lower FRP plates can be neglected if axial stiffness ratio of the concrete-to-plate prism is large enough.

Key words: FRP, interface, bond-slip law, critical length, continuous beam, ultimate load

1 Introduction

The strengthening of concrete structures by means of externally-bonded fibre reinforced polymers (FRPs) is now routinely considered as a viable alternative to the rather costly

* 袁鸿,教授,暨南大学力学与土木工程系。由王宽诚教育基金会资助,于2007年7月赴希腊佩特雷参加“第八届混凝土结构纤维复合材料增强国际会议”,此为其向大会递交的论文。

replacement of these structures. A concrete structure can be strengthened by bonding an FRP

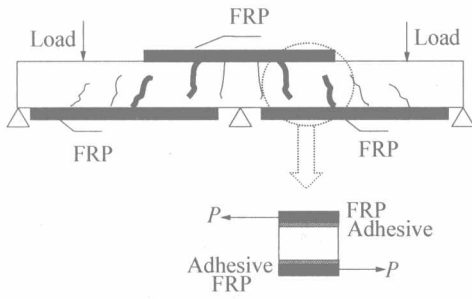


Fig. 1 Continuous beam strengthened by FRP

adjacent main cracks as shown in Fig. 1 may be idealized as the simple model in Fig. 2.

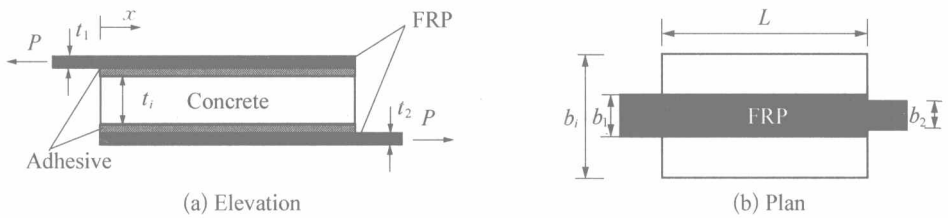


Fig. 2 Mechanics model of FRP strengthening concrete in double surface model

Assume that the width and thickness of each of the five components (two plates, two adhesive layers and concrete prism) are constant along the length. The width of the upper plate, concrete and the lower plate are denoted by b_1 , b_i and b_2 respectively, the thickness of those by t_1 , t_i and t_2 respectively, and the Young's modulus of those are E_1 , E_i and E_2 respectively. The bonded length of the plate (*i. e.* bond length) is denoted by L . The interfacial slip is defined as the relative displacement between the neighboring adherends. The slips of the upper and lower interfaces are denoted by δ_1 and δ_2 respectively. The softening length and debonded length in the interfaces are denoted by a and d respectively.

In such a joint, the adhesive layer is mainly subjected to shear deformations. A simple mechanical model for this joint can be thus established by treating the two plates and the concrete prism (the three adherends) as being subject to axial deformations only while the adhesive layer can be assumed to be subject to shear deformations only. That is, three adherends are assumed to be subject to uniformly distributed axial stresses only, with any bending effects neglected, while the adhesive layer is assumed to be subject to shear stresses only which are also constant across the thickness of the adhesive layer. It should be noted that in such a model, the adhesive layer represents not only the deformation of the actual adhesive layer but also that of the materials adjacent to the adhesive layer and is thus also referred to in the paper as the interface^[2-7].

2 Governing Equations

Based on equilibrium considerations (Fig. 3), the following fundamental equations can be easily found.

$$\frac{d\sigma_1}{dx} + \frac{\tau_1}{t_1} = 0, \quad (1a)$$

$$\frac{d\sigma_2}{dx} - \frac{\tau_2}{t_2} = 0, \quad (1b)$$

$$\sigma_1 t_1 b_1 + \sigma_i t_i b_i + \sigma_2 t_2 b_2 = P. \quad (1c)$$

The constitutive equations for the two adhesive layers (here assume that they have the same properties) and the three adherends can be expressed as

$$\sigma_1 = E_1 \frac{du_1}{dx}, \quad (2a)$$

$$\sigma_i = E_i \frac{du_i}{dx}, \quad (2b)$$

$$\sigma_2 = E_2 \frac{du_2}{dx}, \quad (2c)$$

$$\tau_1 = f(\delta_1), \quad (2d)$$

$$\tau_2 = f(\delta_2). \quad (2e)$$

The interfacial slips of the upper and lower interfaces can be expressed as

$$\delta_1 = u_i - u_1, \quad (3a)$$

$$\delta_2 = u_2 - u_i. \quad (3b)$$

Because of complexity of unsymmetrical model, this paper considers only the symmetrical model for simplicity, *i. e.*, the upper and lower FRP plates have the same materials, thickness and width ($E_1 = E_2, t_1 = t_2, b_1 = b_2$). Substituting Eqs. (1) and (2) into Eq. (3) yield the following governing differential equations:

$$\frac{d^2 \delta_1}{dx^2} = b_1 \left(\frac{1}{E_1 t_1 b_1} + \frac{1}{E_i b_i t_i} \right) f(\delta_1) - \frac{b_1}{E_i b_i t_i} f(\delta_2), \quad (4a)$$

$$\frac{d^2 \delta_2}{dx^2} = b_1 \left(\frac{1}{E_1 t_1 b_1} + \frac{1}{E_i b_i t_i} \right) f(\delta_2) - \frac{b_1}{E_i b_i t_i} f(\delta_1). \quad (4b)$$

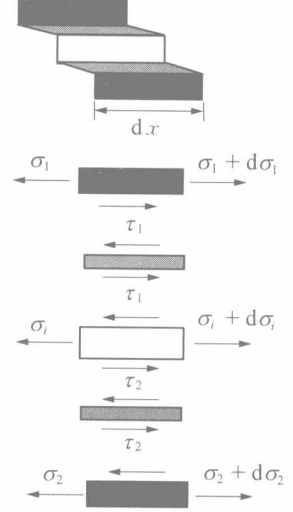


Fig. 3 Deformation and stresses

And the stresses in plates

$$\sigma_1 = E_1 \frac{\frac{P}{E_1 b_1 t_1} - (k+1) \frac{d\delta_1}{dx} - \frac{d\delta_2}{dx}}{2+k}, \quad (5a)$$

$$\sigma_2 = E_1 \frac{\frac{P}{E_1 b_1 t_1} + \frac{d\delta_1}{dx} + (k+1) \frac{d\delta_2}{dx}}{2+k}, \quad (5b)$$

where k is the axial stiffness ratio of the concrete-to-plate prism

$$k = \frac{E_l b_l t_l}{E_1 b_1 t_1}. \quad (6)$$

3 Local Bond-slip Model

Various bond-slip models have been considered in previous work^[2]. However, experimental results^[8] indicate that the bilinear model shown in Fig.4 which features a linear ascending branch followed by a linear descending branch provides a close approximation. According to this model, the bond shear stress increases linearly with the interfacial slip until it reaches the peak stress τ_f at which the value of the slip is denoted by δ_e . Interfacial softening (or micro-cracking) then starts with the shear stress reducing linearly with the interfacial slip. The shear stress reduces to zero when the slip exceeds δ_f , signifying the shear fracture (or debonding or macro-cracking) of a local bond element. This bond-slip model shown in Fig.4 is mathematically described by the following

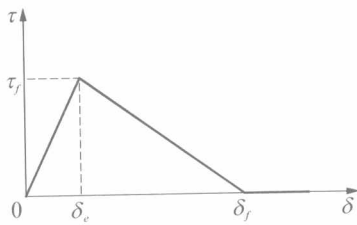


Fig.4 Local bond-slip model

$$\tau = f(\delta) = \begin{cases} \frac{\tau_f}{\delta_e} \delta, & 0 \leq \delta \leq \delta_e, \\ \frac{\tau_f}{\delta_f - \delta_e} (\delta_f - \delta), & \delta_e < \delta \leq \delta_f, \\ 0, & \delta > \delta_f. \end{cases} \quad (7)$$

4 Analysis for Failure Process

Once the bond-slip model is defined, the governing Eq. (4) can be solved to find the shear stress distribution along the interface. The solution is presented below stage by stage with illustrations of the corresponding interfacial shear stress distribution (Fig.5). The solution presented here and the interfacial shear stress distribution shown in Fig.5 is strictly correct only

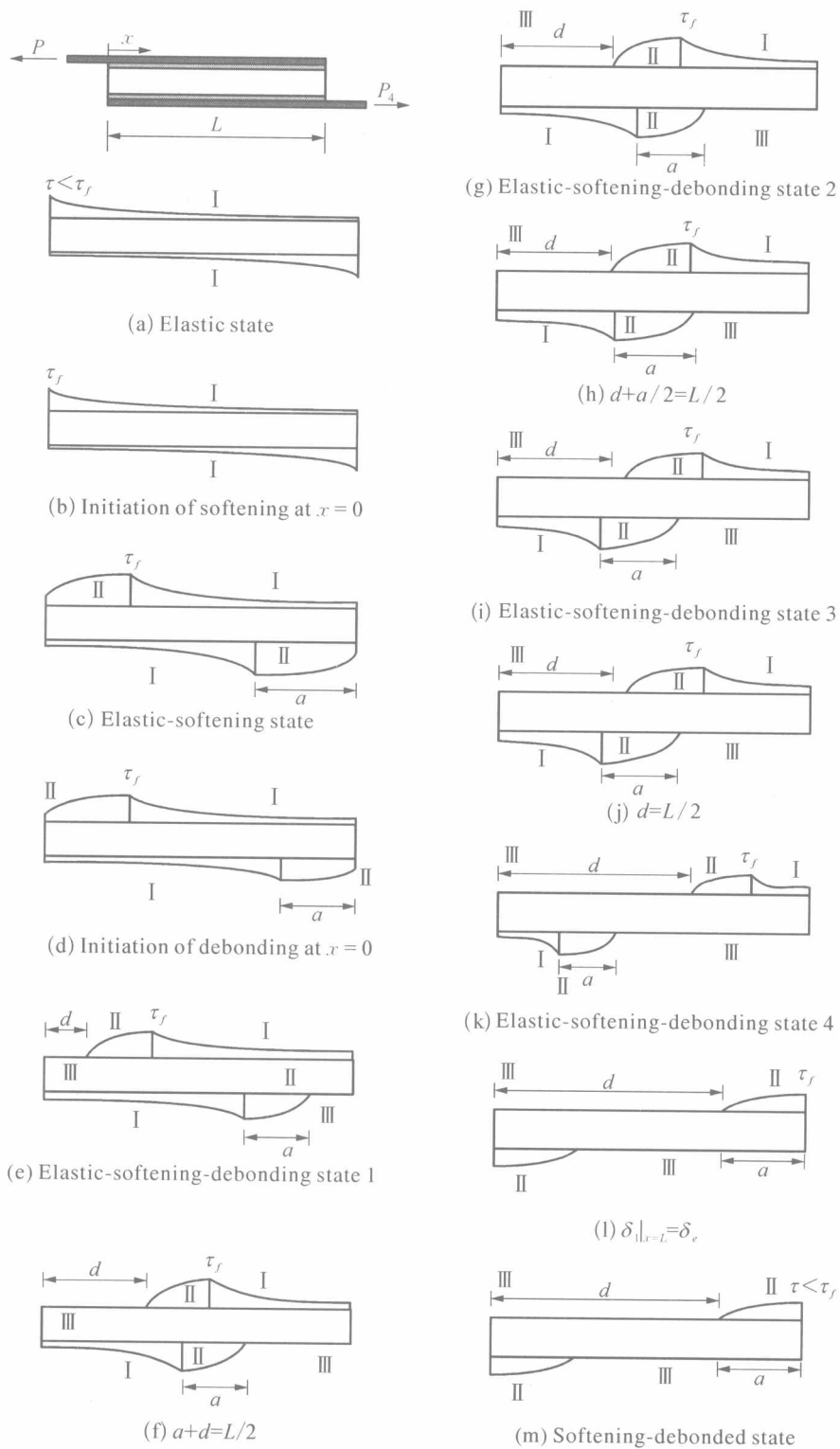


Fig. 5 Interfacial shear stress distribution for each state

for a bond length longer than critical length whose value will be defined in the following. With the increase of P , the interfacial shear stress distribution features an elastic stage, an elastic-softening stage, an elastic-softening-debonded stage which has four sub-stages, and a softening-debonded stage. Therefore, 7 interfacial shear stress states and 6 critical conditions between different interfacial shear stress states will be appeared in the debonding process. Fig. 5 shows the 13 different debonding processes from (a) to (m). (a) elastic state ($\delta_1|_{x=0} < \delta_e$); (b) critical condition between elastic state and elastic-softening state ($\delta_1|_{x=0} = \delta_e$); (c) elastic-softening state ($\delta_e < \delta_1|_{x=0} < \delta_f$); (d) critical condition between elastic-softening state and elastic-softening-debonded state 1 ($\delta_1|_{x=0} = \delta_f$); (e) elastic-softening-debonded state 1 ($a + d < L/2$); (f) critical condition between elastic-softening-debonded state 1 and elastic-softening-debonded state 2 ($a + d = L/2$); (g) elastic-softening-debonded state 2 ($a/2 + d < L/2 < a + d$); (h) critical condition between elastic-softening-debonded state 2 and elastic-softening-debonded state 3 ($a/2 + d = L/2$); (i) elastic-softening-debonded state 3 ($d < L/2 < a/2 + d$); (j) critical condition between elastic-softening-debonded state 3 and elastic-softening-debonded state 4 ($d = L/2$); (k) elastic-softening-debonded state 4 ($\delta_1|_{x=L} < \delta_e$); (l) critical condition between elastic-softening-debonded state 4 and softening-debonded state ($\delta_1|_{x=L} = \delta_e$); (m) softening-debonded state ($\delta_1|_{x=L} > \delta_e$).

4.1 Elastic stage

At small loads, there is no interfacial softening or debonding along the upper and lower plate-to-concrete interfaces. So the entire length of the interfaces is in an elastic stress state (state I) (Fig. 5(a)). This is true as long as the upper interfacial shear stress at $x = L$ is less than τ_f . Since the upper and lower FRP plates have the same materials, thickness and width ($E_1 = E_2, t_1 = t_2, b_1 = b_2$), it can be obtained that $\delta_2(x) = \delta_1(L - x)$ for each stage. Therefore, only half the boundary conditions are needed in deduction. Substituting the relationship of Eq. (7) for the case of $\delta \leq \delta_e$ into Eq. (4), the following differential equations are obtained

$$(D^2 - \lambda_1)\delta_1 + \lambda_2\delta_2 = 0, \quad (8a)$$

$$\lambda_2\delta_1 + (D^2 - \lambda_1)\delta_2 = 0, \quad (8b)$$

where $D = \frac{d}{dx}$, and

$$\lambda_1 = b_1 \left(\frac{1}{E_1 b_1 t_1} + \frac{1}{E_i b_i t_i} \right) \frac{\tau_f}{\delta_e}, \quad (9a)$$

$$\lambda_2 = b_1 \frac{1}{E_i b_i t_i} \frac{\tau_f}{\delta_e}, \quad (9b)$$

and the boundary conditions are

$$\sigma_1 \big|_{x=0} = \frac{P}{b_1 t_1}, \quad (10a)$$

$$\sigma_2 \big|_{x=0} = 0. \quad (10b)$$

With these boundary conditions and symmetry $\delta_2(x) = \delta_1(L-x)$ the following expressions for the interfacial slips are found by solving Eq. (8)

$$\begin{aligned} \delta_1 = & \frac{P}{E_1 t_1 b_1} \frac{1}{2\alpha_1 (1 + e^{-\alpha_1 L})} [e^{-\alpha_1 x} - e^{-\alpha_1 (L-x)}] \\ & + \frac{P}{E_1 t_1 b_1} \frac{1}{2\beta_1 (1 - e^{-\beta_1 L})} [e^{-\beta_1 x} + e^{-\beta_1 (L-x)}], \end{aligned} \quad (11a)$$

$$\begin{aligned} \delta_2 = & -\frac{P}{E_1 t_1 b_1} \frac{1}{2\alpha_1 (1 + e^{-\alpha_1 L})} [e^{-\alpha_1 x} - e^{-\alpha_1 (L-x)}] \\ & + \frac{P}{E_1 t_1 b_1} \frac{1}{2\beta_1 (1 - e^{-\beta_1 L})} [e^{-\beta_1 x} + e^{-\beta_1 (L-x)}], \end{aligned} \quad (11b)$$

where

$$\alpha_1 = \sqrt{\lambda_1 + \lambda_2}, \quad (12a)$$

$$\beta_1 = \sqrt{\lambda_1 - \lambda_2}. \quad (12b)$$

When elastic state is finished, load reaches maximum value P_{\max}^e at this state (Fig. 5(b)). The critical condition between elastic state and elastic-softening state is

$$\delta_1 \big|_{x=0} = \delta_e. \quad (13)$$

Substituting Eq. (13) into Eq. (11a) yield the following

$$P_{\max}^e = \frac{2\delta_e E_1 t_1 b_1}{\frac{1 - e^{-\alpha_1 L}}{\alpha_1 (1 + e^{-\alpha_1 L})} + \frac{1 + e^{-\beta_1 L}}{\beta_1 (1 - e^{-\beta_1 L})}}. \quad (14)$$

4.2 Elastic-softening stage

Once the shear stress along the upper plate-to-concrete interfaces reaches τ_f at $x = 0$ ($\delta_1 \big|_{x=0} = \delta_e$), softening commences at both loaded end of the bonded plate, so part of the plate-to-concrete interface enters the softening state (state II) while the rest remains in the elastic state (state I) as shown in Fig. 5(c). The load P continues to increase as the length of the softening zone a increases. Substituting the relationship given in Eq. (7) into Eq. (4) gives the following for the elastic-softening stage

$$(D^2 - \lambda_1)\delta_1 + \lambda_2\delta_2 = 0 \text{ for } 0 \leq \delta_1 \leq \delta_e \text{ and } 0 \leq \delta_2 \leq \delta_e, \quad (15a)$$

$$\lambda_2\delta_1 + (D^2 - \lambda_1)\delta_2 = 0 \text{ for } 0 \leq \delta_1 \leq \delta_e \text{ and } 0 \leq \delta_2 \leq \delta_e, \quad (15b)$$

$$(D^2 + \lambda_3)\delta_1 + \lambda_2\delta_2 = \lambda_3\delta_f \text{ for } \delta_e < \delta_1 \leq \delta_f \text{ and } 0 \leq \delta_2 \leq \delta_e, \quad (15c)$$

$$\lambda_4\delta_1 - (D^2 - \lambda_1)\delta_2 = \lambda_4\delta_f \text{ for } \delta_e < \delta_1 \leq \delta_f \text{ and } 0 \leq \delta_2 \leq \delta_e, \quad (15d)$$

where

$$\lambda_3 = b_1 \left(\frac{1}{E_1 b_1 t_1} + \frac{1}{E_i b_i t_i} \right) \frac{\tau_f}{\delta_f - \delta_e}, \quad (16a)$$

$$\lambda_4 = b_1 \frac{1}{E_i b_i t_i} \frac{\tau_f}{\delta_f - \delta_e}. \quad (16b)$$

The solutions to Eq. (15) can be derived using symmetrical condition $\delta_2(x) = \delta_1(L - x)$ and the following boundary conditions

$$\sigma_1 \Big|_{x=0} = \frac{P}{b_1 t_1}, \quad (17a)$$

$$\sigma_2 \Big|_{x=0} = 0, \quad (17b)$$

$$\delta_1 \Big|_{x=a^-} = \delta_e, \quad (17c)$$

$$\delta_1 \Big|_{x=a^+} = \delta_e, \quad (17d)$$

$$\sigma_1 \text{ is continuous at } x = a, \quad (17e)$$

$$\sigma_2 \text{ is continuous at } x = a, \quad (17f)$$

$$\delta_2 \text{ is continuous at } x = a. \quad (17g)$$

The solution for the softening-elastic region of the interface [$\delta_e < \delta_1 \leq \delta_f$ and $0 \leq \delta_2 \leq \delta_e$ within $0 \leq x \leq a$] is given by

$$\delta_1 = B_1 e^{-\alpha_2 x} + B_2 e^{\alpha_2 x} + B_3 \cos \beta_2 x + B_4 \sin \beta_2 x + \delta_f, \quad (18a)$$

$$\delta_2 = -\frac{(\alpha_2^2 + \lambda_3)}{\lambda_2} (B_1 e^{-\alpha_2 x} + B_2 e^{\alpha_2 x}) + \frac{(\beta_2^2 - \lambda_3)}{\lambda_2} (B_3 \cos \beta_2 x + B_4 \sin \beta_2 x), \quad (18b)$$

where

$$\alpha_2 = \sqrt{\frac{\lambda_1 - \lambda_3 + \sqrt{(\lambda_1 - \lambda_3)^2 - 4(\lambda_2 \lambda_4 - \lambda_1 \lambda_3)}}{2}}, \quad (19a)$$

$$\beta_2 = \sqrt{\frac{\sqrt{(\lambda_1 - \lambda_3)^2 - 4(\lambda_2 \lambda_4 - \lambda_1 \lambda_3)} - (\lambda_1 - \lambda_3)}{2}}, \quad (19b)$$

and that for the elastic region of the interface $[0 \leq \delta_1 \leq \delta_e \text{ and } 0 \leq \delta_2 \leq \delta_e \text{ within } a < x \leq L - a]$ is given by

$$\delta_1 = B_5 e^{-\alpha_1 x} + B_6 e^{\alpha_1 x} + B_7 e^{-\beta_1 x} + B_8 e^{\beta_1 x}, \quad (20a)$$

$$\delta_2 = -B_5 e^{-\alpha_1 x} - B_6 e^{\alpha_1 x} + B_7 e^{-\beta_1 x} + B_8 e^{\beta_1 x}. \quad (20b)$$

9 unknowns B_1, B_2, \dots, B_8 and a can be determined by the following simultaneous equations

$$B_4 = -\frac{P}{E_1 t_1 b_1} (\alpha_2^2 + \lambda_3) \frac{1}{\beta_2 (\alpha_2^2 + \beta_2^2)}, \quad (21a)$$

$$-B_1 + B_2 = -\frac{P}{E_1 t_1 b_1} (\beta_2^2 - \lambda_3) \frac{1}{\alpha_2 (\alpha_2^2 + \beta_2^2)}, \quad (21b)$$

$$B_6 = -e^{-\alpha_1 L} B_5, \quad (21c)$$

$$B_8 = e^{-\beta_1 L} B_7, \quad (21d)$$

$$B_1 e^{-\alpha_2 a} + B_2 e^{\alpha_2 a} + B_3 \cos \beta_2 a + B_4 \sin \beta_2 a = \delta_e - \delta_f, \quad (21e)$$

$$B_5 [e^{-\alpha_1 a} - e^{-\alpha_1 (L-a)}] + B_7 [e^{-\beta_1 a} + e^{-\beta_1 (L-a)}] = \delta_e, \quad (21f)$$

$$\begin{aligned} & -\frac{\alpha_2^2 + \lambda_3}{\lambda_2} (B_1 e^{-\alpha_2 a} + B_2 e^{\alpha_2 a}) + \frac{\beta_2^2 - \lambda_3}{\lambda_2} (B_3 \cos \beta_2 a + B_4 \sin \beta_2 a) \\ & = -B_5 e^{-\alpha_1 a} - B_6 e^{\alpha_1 a} + B_7 e^{-\beta_1 a} + B_8 e^{\beta_1 a}, \end{aligned} \quad (21g)$$

$$\begin{aligned} -B_1 e^{-\alpha_2 a} + B_2 e^{\alpha_2 a} = & -\frac{\lambda_2}{\alpha_2 (\alpha_2^2 + \beta_2^2)} \left\{ \alpha_1 \left(1 + \frac{\beta_2^2 - \lambda_3}{\lambda_2} \right) [e^{-\alpha_1 a} + e^{-\alpha_1 (L-a)}] B_5 \right. \\ & \left. + \beta_1 \left(\frac{\beta_2^2 - \lambda_3}{\lambda_2} - 1 \right) [e^{-\beta_1 a} - e^{-\beta_1 (L-a)}] B_7 \right\}, \end{aligned} \quad (21h)$$

$$\begin{aligned} -B_3 \sin \beta_2 a + B_4 \cos \beta_2 a = & -\frac{\lambda_2}{\beta_2 (\alpha_2^2 + \beta_2^2)} \left\{ \alpha_1 \left(\frac{\alpha_2^2 + \lambda_3}{\lambda_2} - 1 \right) [e^{-\alpha_1 a} + e^{-\alpha_1 (L-a)}] B_5 \right. \\ & \left. + \beta_1 \left(1 + \frac{\alpha_2^2 + \lambda_3}{\lambda_2} \right) [e^{-\beta_1 a} - e^{-\beta_1 (L-a)}] B_7 \right\}. \end{aligned} \quad (21i)$$

During this stage of loading, debonding (or macrocracking or fracture) commences and propagates along the interface. At the initiation of debonding $\delta_1|_{x=0} = \delta_f$, $a = a_d$ (Fig. 5(d)). It is supposed that L is long enough and $0 \leq \delta_2 \leq \delta_e$ for $x \leq a_d$, that is $L > 2a_d$, then state 1 (Fig. 5(e)) will appear. Substituting $\delta_1|_{x=0} = \delta_f$ into Eq. (18a) yields the following equation which can be used to determine critical length $L_{cr} = 2a_d$ by combining with Eqs. (21)

$$B_1 + B_2 + B_3 = 0. \quad (22)$$

4.3 Elastic-softening-debonding stage

Debonding will appear at elastic-softening-debonding stage. Debonding state is described as state III (Fig. 5). There are 4 different sub-stages in the stage (Fig. 5(e), Fig. 5(g), Fig. 5(i), Fig. 5(k)). At each sub-stage the interface is divided into 5 segments from left to right. Substituting the relationship given in Eq. (7) for different segments into Eq. (4) gives governing equations. The solutions to governing equations can be derived using symmetrical condition $\delta_2(x) = \delta_1(L-x)$ and the corresponding boundary conditions.

4.4 softening-debonded stage

With the continuing loading, peak shear stresses τ_f on upper and lower interface will arrive at the unloaded end as shown in Fig. 5(l) and then the interface enters softening-debonding stage (Fig. 5(m)). Substituting the relationship given in Eq. (7) into Eq. (4) gives governing equations. The solutions to governing equations can be derived using symmetrical condition $\delta_2(x) = \delta_1(L-x)$ and the corresponding boundary conditions.

It is found that the softening length a is a constant as

$$a = \frac{\pi}{2\sqrt{\lambda_3}}. \quad (23)$$

Eq. (23) is the same as in reference [3, 5].

5 Numerical Calculation

To show that how do the upper and lower FRP plates affect each other, the following material and geometric parameters are used in example unless otherwise stated: $t_1 = 0.165$ mm, $b_1 = 25$ mm, $t_i = 150$ mm, $b_i = 150$ mm, $L = 190$ mm, $E_1 = 256$ GPa, $E_i = 28.6$ GPa, $\delta_e = 0.034$ mm, $\delta_f = 0.16$ mm and $\tau_f = 7.2$ MPa.

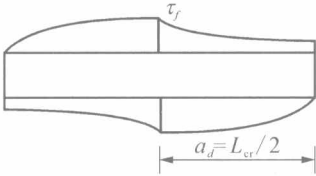


Fig. 6 Critical length $L_{cr} = 2a_d$

5.1 Critical value of bond length

It is supposed that L is long enough in this paper, that is $L \geq 2a_d$. The critical length $L_{cr} = 2a_d$ can be determined by solving Eqs. (21) and (22). It is obtained that $L_{cr} = 2a_d = 101.72$ mm (Fig. 6).

5.2 Effect of stiffness ratio

Axial stiffness ratio of concrete-to-plate prism is denoted by k , that is $k = \frac{E_i b_i t_i}{E_1 b_1 t_1}$. Except